Scientific Research and Essays Vol. 7(27), pp. 2390-2408, 19 July, 2012
Available online at http://www.academicjournals.org/SRE
DOI: 10.5897/SRE12.176
ISSN 1992-2248 ©2012 Academic Journals

Full Length Research Paper

Nonlinear analysis of frames composed of flexibly connected members with rigid end sections accounting for shear deformations

Halil Gorgun*, Senem Yilmaz and Seval Sevgi Karacan

Department of Civil Engineering, Dicle University, 21280, Diyarbakir, Turkey.

Accepted 20 June, 2012

The behaviour of lintel beam-to-shear wall connections plays an important role in the analysis of shear walls with openings. A computer-based method was prepared for nonlinear frames comprised of lintel beams having fully rigid end sections flexibly connected to wide column members accounting for shear deformations. The analytical procedure employed stability functions to model the effect of axial force on the stiffness of members. The modified member stiffness matrix and the fixed end forces for various loads were found. The nonlinear analysis method was applied for a model shear wall problem. The method is readily implemented on a computer using matrix structural analysis techniques and is applicable for the efficient nonlinear analysis of frameworks.

Key words: Nonlinear analysis, semi-rigid connection, shear deformation, shear wall, lintel beam.

INTRODUCTION

The effects of both geometrical and material nonlinearities and the semi-rigid connections on the overall behaviour of framed structures have attracted a great deal of attention from designers and researchers in recent years. These nonlinear effects are particularly important for the design of certain type of structures.

When designing frames it is customary to assume that joints are either:

(i) pinned-implying no moment transfer, or
(ii) rigid-implying complete rotational continuity.

The notions of either pinned or rigid joints are, however, simply extreme cases of true joint behaviour, and experimental investigations, many of which are referred to by Jones et al. (1983), show clearly that actual joints exhibit characteristics over a wide spectrum between these extremes. The models with ideal connections simplify analysis procedure, but often cannot represent real structural behaviour. This discrepancy is reported in numerous experimental investigations of steel frames with different types of connections. The rigid connection idealization indicates that relative rotation of the connection does not exist and the end moment of the beam is entirely transferred to the columns. In contrast to the rigid connection assumption, the pinned connection idealization indicates that any restraint does exist for rotation of the connection and the connection moment is zero. Although these idealizations simplify the analysis and design process, the predicted response of the frame may be different from its real behaviour. Therefore, this idealization is not adequate as all types of connections are more or less, flexible or semi-rigid. It is proved by numerous experimental investigations that have been carried out in the past (Moree et al., 1993). The term semi-rigid is used to express the real connection behaviour. Therefore, beam-to-column connections in the analysis/design of frames should be described as semi-rigid connections.

Generally, nodal connections of plane frames are subjected to influence of bending moments, axial forces

*Corresponding author. E-mail: hgorgun@dicle.edu.tr. Tel: +90 412 248 8402. Fax: +90 412 248 8405.

and shear forces. The effects of axial and shear forces can usually be ignored, and only the influence of bending moments is of practical interest. The constitutive moment-relative rotation relation, M-ϕ, depends on the particular type of connection. Most experiments have shown that the M-ϕ curve is nonlinear all the whole domain and for all types of connections. Therefore, modelling of the nodal connection is very important for the analysis and design of frame structure.

Based on experimental work due to static monotonic loading tests carried out for various types of beam-to column connections, many models have been suggested to approximate the connection behaviour. The simplest and the most common one is the linear model that has been broadly used for its simplicity (Monforton and Wu, 1963; Gorgun, 1992; Chan and Zhau, 1994). This approach is based on modelling the connection as a lengthless rotational spring. This method is widely used in semi-rigid analysis of frames, and the implementation of this approach requires small modifications in the existing analysis programs. This modification doe not considerably increase the computational time. Therefore, each element of the frame consists of a finite length element with a lengthless rotational spring. However, this model is good only for the low level loads, when the connection and member moments are quite small. In each other case, when the connection and member rigidities decrease compared with its initial values, a nonlinear material model is necessary. Several mathematical models to describe the nonlinear behaviour of connections and materials have been formulated and widely used in research practice (Wu and Chen, 1990). Often, many authors use the so called corrective matrices to modify the conventional stiffness matrices of the beams with fully fixity at both ends (Romstad and Subramanian, 1970; Frye and Morris, 1975; Yu and Shanmugam, 1986). Elements of the corrective matrices are functions of the particular nondimensional parameters-fixity factors, or rigidity index. In Simoes (1996), such an approach is used in the context of the optimization of steel frames with semi-rigid connections.

In addition to the linear behaviour, many studies have been developed to the nonlinear analysis of the static and dynamic behaviour of frames with semi-rigid connections using different models of geometrical and material nonlinearities of elements and nodal connections (Sekulovic et al., 2002; Kameshki and Saka, 2003). In most studies, the effect of shear deformation and axial force on elastic behaviour has been ignored as being of little consequence. However, there are steel frameworks for which shear effects may be significant (for example, those that have deep transfer girders (Hall and Newmark, 1957; Dincer, 1989; Timoshenko and Gere, 1961; Aristizabal-Ochoa, 2012). Also, in the analysis of structural systems the members forming the planar frames are generally assumed to be rigidly connected among each other. However, more often than not the assumption of pin connections is also employed in such cases where the rigidity of the connection cannot be provided to a dependable degree. In fact, both of the foregoing assumptions are unrealistic when one is treating steel frames and especially, nowadays, widely used precast reinforced concrete structures. In such structures beams and columns behave as if they are semi-rigidly, or flexibly, connected among themselves, as far as the rotations of the ends are concerned. Hence, experimentally determined effective rotational spring constants for those connections should be used in the analyses of such structures. This paper presents a computer-based method for geometrically and materially nonlinear analysis of planar frameworks with semi-rigid connections based on Timoshenko beam theory so as to explicitly account for the influence of shear deformation and the axial force on elastic behaviour (Timoshenko and Gere, 1961). Stability functions are employed to model the effect of axial force on the elastic bending stiffness of members, and the influence of semi-rigid connections is taken into account. The shear-stiff stability functions presented in Livesley and Chandler (1956) and Chen and Lui (1991) are modified to take shear deformability into account. The history of the stability functions for shear-flexible members is given in Al-Sarraf (1986) and Mottram (2008).

The geometrically and materially nonlinear elastic analysis procedure is a direct extension of the conventional matrix displacement method of linear-elastic analysis. The nonlinear analysis method is verified for an example structure from the literature (Dincer, 1989).

The present study is an attempt to prepare a computer program that treats the aforementioned type of structures elegantly, taking into consideration the behaviour of the flexible connections, rigid end sections and the influence of shear deformations on elastic behaviour along with the effect of geometrical and material nonlinearities due to the axial forces in the members. As is well known, the upper limit of the load in any structure is the critical value of the load, the buckling load, which is found by taking geometric and material nonlinearities into consideration. Hence, the results of the present study will constitute the basis of the stability analysis of the same type of structures.

In the present study a thorough analysis of planar frames and pierced shear walls has been carried out using the well-known stiffness method of structural analysis and a second order approach with material nonlinearity, taking into consideration, not only the effects of bending and axial deformations, but also those due to shear as well. The geometrical nonlinear analysis of plane frame in literatures is extended in this study to include the material nonlinearity. The section properties used for the formation of the stiffness matrix should also be updated using the effective section properties $(EI)_{eff}$ and $(EA)_{eff}$. First, the stiffness matrix of a member elastically supported against rotation at both ends having rigid end sections is obtained using the second order analysis. Then, the fixed end forces are found for a member elastically supported at the two ends by rotational springs for a uniformly distributed load, a concentrated load, a linearly distributed load, a symmetrical trapezoidal distributed load and an unsymmetrical triangular distributed load. For the latter analysis, the second order theory was employed once again, along with the use of differential equations which yielded trigonometric functions for the case of axial compressive force and hyperbolic functions for the case of axial tensile force.

A computer program has been prepared for applications. Results found in the literature by other methods have been obtained by a straightforward application of this computer program and there is a perfect match between the results of previous studies and those of the present one.

The computer program that was prepared can be used to solve static problems of planar frames composed of members that are flexibly connected at the nodes having rigid end sections.

ANALYSIS MODEL

The present study concerns planar frameworks discretized as an assembly of beam-column members that beams having rigid end sections, flexibly connected to columns taking into account the effect of shear and axial deformations. It is assumed that there are no out-of-plane actions, and bending, shearing or axial deformation (ϕ, γ or δ) under the action of moment, shear or axial force (*M*, *V* or *P*) is concentrated at member sections.

This study is mainly composed of two parts. The first part is comprised of the analytical study that employs the matrix method which is commonly used in structural analysis. In this part, the stiffness matrix of the structure of concern is obtained, the contributions of different types of loads to the loading vector are found and the formulation of the equilibrium equations for the determination of the unknown displacements is explained. Actually, besides the more complicated type of functions compared to linear analysis, there is also a need for separate analyses for compressive and tensile axial forces which doubles the analytical work. In the second part of the study the pertinent computer program was prepared.

In the present study, the method used being the matrix stiffness method the main concern is to set up the relation between the loading and the displacement vectors of a given structure.

To accomplish this, the first thing to be done is to find the relation between the end forces and the end deflections for a prismatic planar beam-column member. The terms “force” and “deflection” are taken to be general expressions signifying direct forces and moments, and linear deflections and rotations respectively. Towards this end we must first define the sign convention and notation which is done in Figure 1a and b where positive senses of the entities at the two ends in the axial, transverse and rotational directions are shown with the arrows numbered from one to six. The left and the right ends of the member are also shown along with the corresponding spring constants, which express the ratio of flexural stiffness of connection to flexural stiffness of beam to which it is attached. The lengths of the springs are supposed to be zero. The physical properties of the member are designated in the conventional manner-*E*, *G*, *L*, *I*, *A* and A_s denote Young’s modulus, shear modulus, length, cross-sectional moment of inertia, cross-sectional area and equivalent shear area respectively; while p_i, d_i and f_i ($i=1$, 2,…, 6) are local axis member-end forces, deformations and fixed end forces, respectively. k_1 and k_2 are the constants of the rotational springs at the left and the right ends, respectively, The member is perfectly straight, and uniform in cross-section throughout its length. The material of the member is linearly elastic.

Modified stiffness matrix of a flexibly connected member

In order to obtain a force-displacement relationship of a beam-column member with semi-rigid connections, the superposition method cannot be applied. The force-deformation relationship for the beam-column member in Figure 1a and b is:

$$p = kd + f \qquad (1)$$

Where the vectors of end-section forces $p=\left[p_1, p_2, \ldots p_6\right]^T$, deformations $d=\left[d_1, d_2, \ldots d_6\right]^T$ and fixed end forces due to intermediate loads between joints $f=\left[f_1, f_2, \ldots f_6\right]^T$ are referenced to the local-axis system for the member, and the local-axis stiffness matrix k for the member is a six by six matrix. The shear contribution in the entire deflection of a beam element as treated in the ordinary small deflection elastic theory is very simple; and, it is very small compared with the flexural deflection. Letting $y = y_m + y_s$ show the entire downwards deflection of a beam-column member in Figure 2, the deflection due to bending only is shown by y_m and that due to shear is shown by y_s, and x show the distance from the left end of the member, one can find the different elements of the stiffness matrix by taking each and every end displacement to be unity at a time, when the others are zero and solving the differential equation.

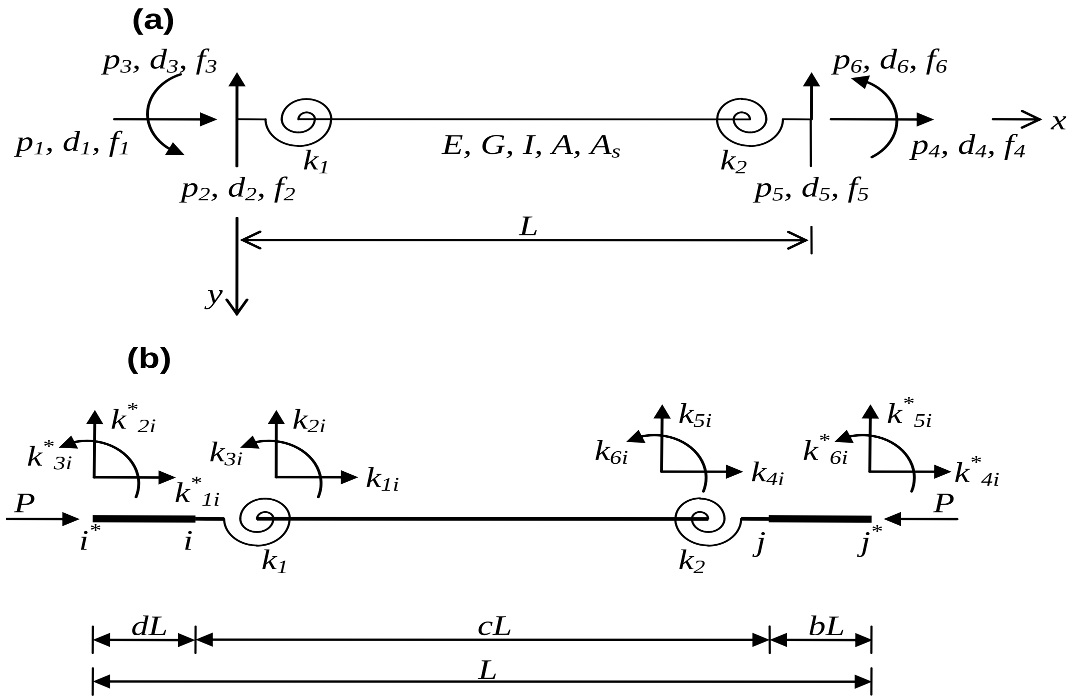

Figure 1. (a) Beam-column member model and (b) Beam-column member model with rigid end sections.

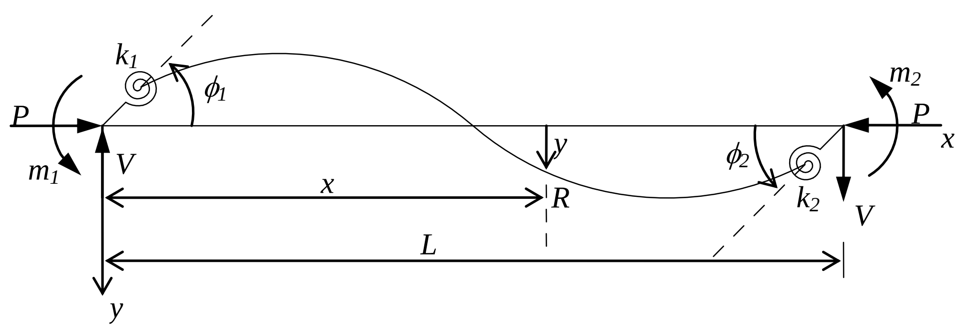

Figure 2. Directions and positive senses of various end properties.

$$y'' = y''_m + y''_s = -\frac{M}{EI\left(1 - P/GA_s\right)} \tag{2}$$

Where a prime shows a derivative with respect to x and EI is the flexural rigidity of the member.

When there is an axial force P, the bending moment M at some representative point R in Figure 2, distant x from the left-hand end:

$$M = \pm Py + Vx - m_1 \tag{3}$$

Where P is the absolute value of the axial force in the member and the sign in front of it in equation (3) is positive for compression and negative for tension, V is the end shear force, m_1 is the modified fixed end moment at $x = 0$, defining:

$$\alpha = \begin{cases} \sqrt{\dfrac{P/EI}{\left(1 - P/GA_s\right)}} & P < 0 \\ \sqrt{\dfrac{P/EI}{\left(1 + P/GA_s\right)}} & P > 0 \end{cases} \tag{4}$$

The general solution of equation (2) is:

$$y = A\sin(\alpha x) + B\cos(\alpha x) - \frac{V}{P}x + \frac{m_1}{P} \quad (5)$$

for axial compressive force.

When the axial force is tensile and the first term in the bending moment expression in equation (3) changes sign, then the general solution of equation (2) is again given by equation (5) only changing the signs of the last two terms and the trigonometric functions to their corresponding hyperbolic ones. Assigning the unit end displacements to the outer ends of the springs, each at a time and using the equilibrium equations for the free body diagrams of the members along with equation (5) and the suitable boundary conditions for the displacements and slopes at the inner ends of the springs, the local–axis stiffness matrix for the member is:

$$k = \begin{bmatrix} k_{11} & 0 & 0 & k_{14} & 0 & 0 \\ & k_{22} & k_{23} & 0 & k_{25} & k_{26} \\ & & k_{33} & 0 & k_{35} & k_{36} \\ & & & k_{44} & 0 & 0 \\ & Sym & & & k_{55} & k_{56} \\ & & & & & k_{66} \end{bmatrix} = \begin{bmatrix} k_{11} & 0 & 0 & -k_{11} & 0 & 0 \\ 0 & k_{22} & k_{23} & 0 & -k_{22} & k_{26} \\ 0 & k_{23} & k_{33} & 0 & -k_{23} & k_{36} \\ -k_{11} & 0 & 0 & k_{11} & 0 & 0 \\ 0 & -k_{22} & -k_{23} & 0 & k_{22} & -k_{26} \\ 0 & k_{26} & k_{36} & 0 & -k_{26} & k_{66} \end{bmatrix} \quad (6)$$

The effects of the flexible connections are included in the stiffness matrix by modifying the stiffness terms of frame member with rigid connections. The stiffness influence coefficients $k_{ij}\left(i=1,2,...6 : j=1,2,...6\right)$ in equation (6) take into account the influence that axial force, shear deformations, rigid end sections, and semi-rigid connections have on elastic bending stiffness and are defined as follows (detailed derivations are given in equation 36):

$$k_{11} = k_{11}^{a} = \frac{EA}{L} = k_{44} = -k_{14} = -k_{41} \quad (7a)$$

$$k_{22} = k_{22}^{r} = \frac{EI\chi_1}{L^3\Omega} = k_{55} = -k_{25} = -k_{52} \quad (7b)$$

$$k_{23} = k_{23}^{r} = \frac{EI\chi_2}{L^2\Omega} = k_{32} = -k_{35} = -k_{53} \quad (7c)$$

$$k_{26} = k_{26}^{r} = \frac{EI\chi_3}{L^2\Omega} = k_{62} = -k_{56} = -k_{65} \quad (7d)$$

$$k_{33} = k_{33}^{r} = \frac{EI\chi_4}{L\Omega} \quad (7e)$$

$$k_{36} = k_{36}^{r} = \frac{EI\chi_5}{L\Omega} = k_{63} \quad (7f)$$

$$k_{66} = k_{66}^{r} = \frac{EI\chi_6}{L\Omega} \quad (7g)$$

the modified local–axis stiffness matrix for the member is,

$$k = \begin{bmatrix} \frac{EA}{L} & 0 & 0 & -\frac{EA}{L} & 0 & 0 \\ 0 & \frac{EI\chi_1}{L^3\Omega} & \frac{EI\chi_2}{L^2\Omega} & 0 & -\frac{EI\chi_1}{L^3\Omega} & \frac{EI\chi_3}{L^2\Omega} \\ 0 & \frac{EI\chi_2}{L^2\Omega} & \frac{EI\chi_4}{L\Omega} & 0 & -\frac{EI\chi_2}{L^2\Omega} & \frac{EI\chi_5}{L\Omega} \\ -\frac{EA}{L} & 0 & 0 & \frac{EA}{L} & 0 & 0 \\ 0 & -\frac{EI\chi_1}{L^3\Omega} & -\frac{EI\chi_2}{L^2\Omega} & 0 & \frac{EI\chi_1}{L^3\Omega} & -\frac{EI\chi_3}{L^2\Omega} \\ 0 & \frac{EI\chi_3}{L^2\Omega} & \frac{EI\chi_5}{L\Omega} & 0 & -\frac{EI\chi_3}{L^2\Omega} & \frac{EI\chi_6}{L\Omega} \end{bmatrix} \quad (7h)$$

In equation (7a), $k_{11}^{a} = EA/L$ is elastic axial stiffness. In equations 7b to g, the stiffness influence coefficients; when axial force P vanishes (linear solution), $P = 0$

$$k_{22}^{r} = \frac{12EI}{L^3\Omega}\left\{1+\beta_1+\beta_2\right\} \quad (8)$$

$$k_{23}^{r} = \frac{6EI}{L^2\Omega}\left(1+2\beta_2\right) \quad (9)$$

$$k_{26}^{r} = \frac{6EI}{L^2\Omega}\left(1+2\beta_1\right) \quad (10)$$

$$k_{33}^{r} = \frac{4EI}{L\Omega}\left\{1+3\left(\beta+\beta_2\right)\right\} \quad (11)$$

$$k_{36}^{r} = \frac{2EI}{L\Omega}\left(1-6\beta\right) \quad (12)$$

$$k_{66}^{r} = \frac{4EI}{L\Omega}\left\{1+3\left(\beta+\beta_1\right)\right\} \quad (13)$$

for the case of axial compressive force, $P < 0$,

$$k_{22}^{r} = \frac{EI}{L^3\Omega}\psi^3\delta^2\left\{\left(1-\psi^2\beta_1\beta_2\right)\sin\psi + \psi\left(\beta_1+\beta_2\right)\cos\psi\right\} \quad (14)$$

$$k_{23}^{r} = \frac{EI}{L^2\Omega}\psi^2\delta\left(\psi\beta_2\sin\psi - \cos\psi + 1\right) \quad (15)$$

$$k_{26}^{r} = \frac{EI}{L^2\Omega}\psi^2\delta\left(\psi\beta_1\sin\psi - \cos\psi + 1\right) \quad (16)$$

$$k_{33}^{r} = \frac{EI}{L\Omega}\psi\left\{\left(1+\psi^2\delta\beta_2\right)\sin\psi - \psi\delta\cos\psi\right\} \quad (17)$$

$$k_{36}^{r} = \frac{EI}{L\Omega}\psi\left(\psi\delta - \sin\psi\right) \quad (18)$$

$$k_{66}^{r} = \frac{EI}{L\Omega}\psi\left\{\left(1+\psi^{2}\delta\beta_{1}\right)\sin\psi - \psi\delta\cos\psi\right\} \quad (19)$$

and for the case of axial tensile force; $P > 0$,

$$k_{22}^{r} = \frac{EI}{L^{3}\Omega}\psi^{3}\delta^{2}\left\{\left(1+\psi^{2}\beta_{1}\beta_{2}\right)\sinh\psi + \psi\left(\beta_{1}+\beta_{2}\right)\cosh\psi\right\} \quad (20)$$

$$k_{23}^{r} = \frac{EI}{L^{2}\Omega}\psi^{2}\delta\left(\psi\beta_{2}\sinh\psi + \cosh\psi - 1\right) \quad (21)$$

$$k_{26}^{r} = \frac{EI}{L^{2}\Omega}\psi^{2}\delta\left(\psi\beta_{1}\sinh\psi + \cosh\psi - 1\right) \quad (22)$$

$$k_{33}^{r} = -\frac{EI}{L\Omega}\psi\left\{\left(1-\psi^{2}\delta\beta_{2}\right)\sinh\psi - \psi\delta\cosh\psi\right\} \quad (23)$$

$$k_{36}^{r} = -\frac{EI}{L\Omega}\psi\left(\psi\delta - \sinh\psi\right) \quad (24)$$

$$k_{66}^{r} = -\frac{EI}{L\Omega}\psi\left\{\left(1-\psi^{2}\delta\beta_{1}\right)\sinh\psi - \psi\delta\cosh\psi\right\} \quad (25)$$

account for elastic bending stiffness.

In equations 8 to 25, the parameters:

$$\beta = \frac{EI}{L^{2}GA_{s}} \quad (26)$$

$$\beta_{1} = \frac{1}{4k_{1}} \quad (27)$$

$$\beta_{2} = \frac{1}{4k_{2}} \quad (28)$$

$$\Omega = \begin{cases} 1+12\beta\left(1+\beta_{1}+\beta_{2}\right)+4\left(\beta_{1}+\beta_{2}+3\beta_{1}\beta_{2}\right) & P=0 \\ \psi\left\{\delta\left(\psi^{2}\beta_{1}\beta_{2}-1\right)+\beta_{1}+\beta_{2}\right\}\sin\psi - \left\{2+\psi^{2}\delta\left(\beta_{1}+\beta_{2}\right)\right\}\cos\psi + 2 & P<0 \\ \psi\left\{\delta\left(\psi^{2}\beta_{1}\beta_{2}+1\right)-\beta_{1}-\beta_{2}\right\}\sinh\psi - \left\{2-\psi^{2}\delta\left(\beta_{1}+\beta_{2}\right)\right\}\cosh\psi + 2 & P>0 \end{cases} \quad (29)$$

in which,

$$\psi = \begin{cases} L\sqrt{\dfrac{P/EI}{\left(1-P/GA_{s}\right)}} & P<0 \\ L\sqrt{\dfrac{P/EI}{\left(1+P/GA_{s}\right)}} & P>0 \end{cases} \quad (30a)$$

$$\delta = \begin{cases} 1-P/GA_{s} & P<0 \\ 1+P/GA_{s} & P>0 \end{cases} \quad (30b)$$

are well-known stability functions that account for the influence of axial force on elastic bending stiffness. The effect of axial forces on the deformed shape of the member are included in the stiffness matrix by using modified stability functions.

Finally, in equations 27 and 28, the dimensionless parameters for the ends, 1 and 2, of the member,

$$k_{1} = \frac{J_{1}}{4EI/L} \quad (31)$$

$$k_{2} = \frac{J_{2}}{4EI/L} \quad (32)$$

Where J_1 and J_2 are the rotational stiffness of the flexible connections at the ends of the member and $4EI/L$ is the stiffness of the member (defined only as the moment required to cause unit rotation of one of its ends).

$$J = \frac{M}{\phi} \quad (33)$$

This assumes a linear moment-rotation relationship and the connection stiffness, J, is the slope of this relationship. The values of k_1 and k_2 depend on the known semi-rigid connection stiffness and the geometrical and elastic properties of the connected member. They vary from zero for a frictionless pin connection to infinity for a perfectly rigid connection. Equations (31) and (32) are for the general case of unequal connection stiffness. Usual steel building frames will have identical connections at both girder ends, although exterior and interior connections may act differently, and the analysis will then deal with equal stiffnesses, $J = J_1 = J_2$.

Modified stiffness matrix of a member with rigid end sections

Shear walls are usually connected by beams and for the purposes of analysis we have to find the stiffness of such a beam corresponding to coordinates at the wall axis. In the simplified analysis, walls with a row of openings are idealised to a frame composed of two wide columns connected by beams with end parts infinitively rigid. Consider the beam *i*j** of Figure 1b. We assume that the beam has two rigid parts *i*i* and *j*j.* The rotations at the wall axis and at the other end of the rigid part will be the same. Also because of rigid part axial displacements should be the same for each end. Rigid part will have rigid-body movement. Here it is assumed that the relative rotation of the beam and the wall face at the joint would not be zero.

In the present study all four kinds of the abovementioned properties are treated at the same time, namely, rigid end sections, second order effects, the effects of shear deformations, and the effects of semi-rigid connections. Figure 1b shows a member with rigid end sections and semi-rigid connections. Here, *i** and *j** show the ends of the member including the rigid end sections. They represent the points on the axes of the high beams or wide shear walls on the two sides of the member. *i* and *j* show the points where the elastic part of the member ends, representing the points on the surface of the high beams and wide shear walls where semi-rigid connections take place. The rotations and the translations, parallel to the axis of the member, at the ends of either rigid section are equal to each other. Hence, it can easily be proved that the stiffness matrix of member *i*j** is also symmetrical and its elements which are different from those of member *ij* can be found as follows:

$$k^* = \begin{bmatrix} k_{11} & 0 & 0 & -k_{11} & 0 & 0 \\ 0 & k_{22} & k_{23}^* & 0 & -k_{22} & k_{26}^* \\ 0 & k_{23}^* & k_{33}^* & 0 & -k_{23}^* & k_{36}^* \\ -k_{11} & 0 & 0 & k_{11} & 0 & 0 \\ 0 & -k_{22} & -k_{23}^* & 0 & k_{22} & -k_{26}^* \\ 0 & k_{26}^* & k_{36}^* & 0 & -k_{26}^* & k_{66}^* \end{bmatrix} \tag{34a}$$

$$k_{23}^* = k_{23} + k_{22}\left(dL\right) = k_{32}^* = -k_{35}^* = -k_{53}^* \tag{34b}$$

$$k_{26}^* = k_{26} + k_{22}\left(bL\right) = k_{62}^* = -k_{56}^* = -k_{65}^* \tag{34c}$$

$$k_{33}^* = k_{33} + 2k_{23}\left(dL\right) + k_{22}\left(dL\right)^2 \pm P\left(dL\right) \tag{34d}$$

$$k_{36}^* = k_{36} + k_{23}\left(bL\right) + k_{26}\left(dL\right) + k_{22}\left(dL\right)\left(bL\right) = k_{63}^* \tag{34e}$$

$$k_{66}^* = k_{66} + 2k_{26}\left(bL\right) + k_{55}\left(bL\right)^2 \pm P\left(bL\right) \tag{34f}$$

Where P is the absolute value of the axial force in the member and the sign in front of it in equations (34d) and (34f) is positive for tension, negative for compression, and vanishes ($P=0$) for linear solution.

Modified fixed end moments with semi-rigid connections

So far only structures loaded at joints have been considered, but in rigid jointed structures this is generally not the case. In order to deal with this problem, the whole solution process must be reviewed. In the analysis of skeletal structures by the stiffness method it was observed that the loading vector might contain fixed-end forces due to loads applied between joints. It is found that the presence of an axial load, shear force, and the influence of semi-rigid connections in a member affects the values of the fixed-end forces, and this is summarised in this section.

Concerning fixed end forces for numerous types of span loadings, although the computations involved are rather tedious, the method of approach is straightforward and simple. What needs to be done in each case is to employ the method used for finding the stiffness matrix, namely apply equation (2) where bending moment M given by equation (3), is expressed with an additional term or terms due to the span loading and the force V at the left end is found by using the moment equilibrium equation relative to the right end. Moreover, for the case of symmetrical trapezoidal distributed load, by making use of symmetry, the mid-span slope was taken to be zero. The corresponding transverse forces can be found by making use of the two equations of equilibrium for the member. The moments at the elastically restrained ends of a loaded member for some frequently encountered loads found for linear and nonlinear cases are presented as follows with the notation given in the relative figures and detailed derivations are given in Yilmaz (2008).

Uniformly distributed load

Figure 3 shows an elastically restrained member of length *L* and uniform flexural rigidity of section *EI*, loaded with a uniformly distributed load of intensity *w* per unit length over the whole span. The modified fixed end moments on the member ends due to a uniform downward load, *w*, are:

$$m_1 = \begin{cases} \dfrac{wL^2}{12\Omega}\left(1+12\beta+6\beta_2\right) & P=0 \\ \dfrac{wL^2\left(1+\psi^2\beta\right)}{2\psi^2\Omega}\Big\{\psi\left[4+\psi^2\left(2\beta+\beta_2\right)\right]\sin\psi & \\ +\left[4-\psi^2\left(1-4\beta-2\beta_2\right)\right]\cos\psi-\left[4+\psi^2\left(1+4\beta+2\beta_2\right)\right]\Big\} & P<0 \\ -\dfrac{wL^2\left(1-\psi^2\beta\right)}{2\psi^2\Omega}\Big\{\psi\left[4-\psi^2\left(2\beta+\beta_2\right)\right]\sinh\psi & \\ -\left[4+\psi^2\left(1-4\beta-2\beta_2\right)\right]\cosh\psi+\left[4-\psi^2\left(1+4\beta+2\beta_2\right)\right]\Big\} & P>0 \end{cases} \tag{35a}$$

$$m_2 = -\begin{cases} \dfrac{wL^2}{12\Omega}\left(1+12\beta+6\beta_1\right) & P=0 \\ \dfrac{wL^2\left(1+\psi^2\beta\right)}{2\psi^2\Omega}\Big\{\psi\left[4+\psi^2\left(2\beta+\beta_1\right)\right]\sin\psi & \\ +\left[4-\psi^2\left(1-4\beta-2\beta_1\right)\right]\cos\psi-\left[4+\psi^2\left(1+4\beta+2\beta_1\right)\right]\Big\} & P<0 \\ \dfrac{wL^2\left(1-\psi^2\beta\right)}{2\psi^2\Omega}\Big\{\psi\left[4-\psi^2\left(2\beta+\beta_1\right)\right]\sinh\psi & \\ +\left[4+\psi^2\left(1-4\beta-2\beta_1\right)\right]\cosh\psi-\left[4-\psi^2\left(1+4\beta+2\beta_1\right)\right]\Big\} & P>0 \end{cases} \tag{35b}$$

Concentrated load at any point

Modified fixed end moments in the same uniform member

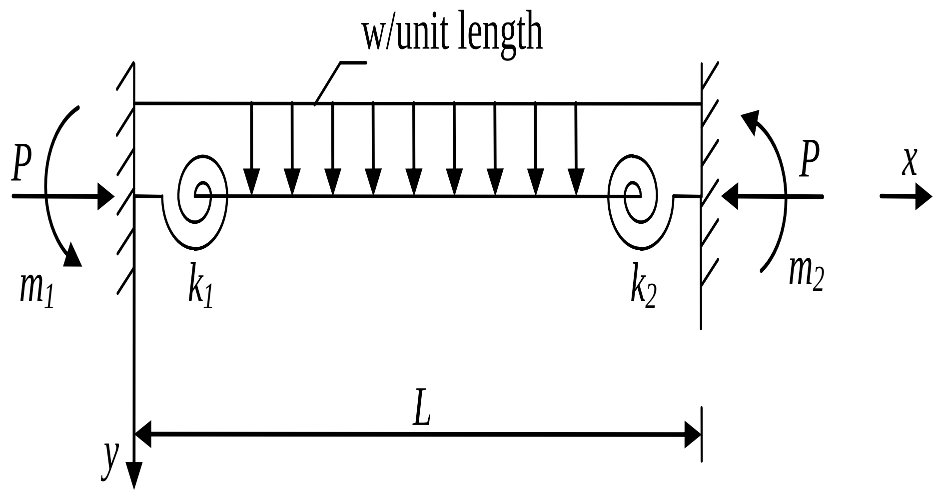

Figure 3. Uniformly distributed load.

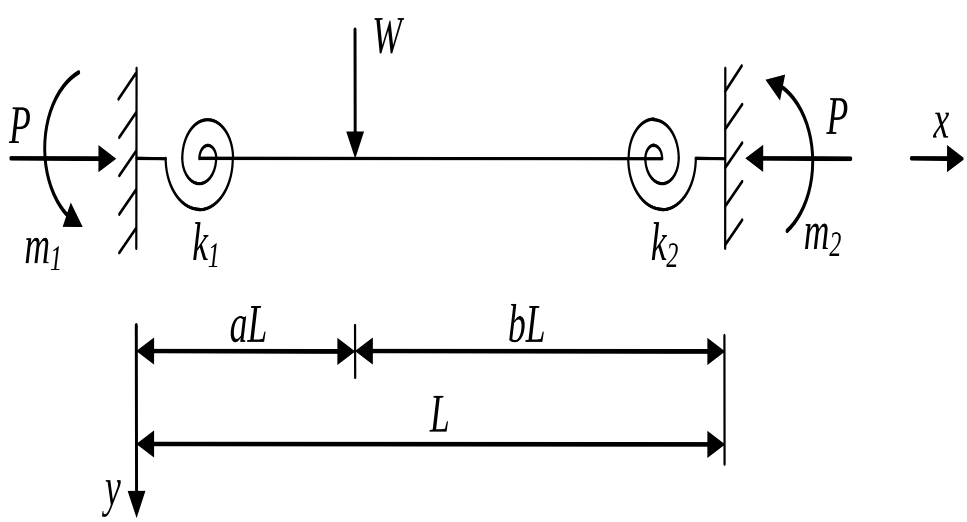

Figure 4. Single-point load.

of length L by an unsymmetrical point load of W as shown in Figure 4.

$$m_1 = \begin{cases} WLa\dfrac{b\left\{b+2\beta_2\left(b+1\right)\right\}}{1+4\left(\beta_1+\beta_2+3\beta_1\beta_2\right)} & P=0 \\ \dfrac{WL}{\psi\Omega}\left\{\left(1+\psi^2\beta\right)\left(\left(1+\psi^2\left(\beta+b\beta_2\right)\right)\sin\psi-b\psi\cos\psi-\sin a\psi-a\psi\right)\right. & \\ \left.-\left(1+\psi^2\left(\beta+\beta_2\right)\right)\sin b\psi+\psi\cos b\psi\right\} & P<0 \\ -\dfrac{WL}{\psi\Omega}\left\{\left(1-\psi^2\beta\right)\left(\left(1-\psi^2\left(\beta+b\beta_2\right)\right)\sinh\psi-b\psi\cosh\psi-\sinh a\psi-a\psi\right)\right. & \\ \left.-\left(1-\psi^2\left(\beta+\beta_2\right)\right)\sinh b\psi+\psi\cosh b\psi\right\} & P>0 \end{cases} \tag{36a}$$

$$m_2 = -\begin{cases} WLb\dfrac{a\left\{a+2\beta_1\left(a+1\right)\right\}}{1+4\left(\beta_1+\beta_2+3\beta_1\beta_2\right)} & P=0 \\ \dfrac{WL}{\psi\Omega}\left\{\left(1+\psi^2\beta\right)\left(\left(1+\psi^2\left(\beta+a\beta_1\right)\right)\sin\psi-a\psi\cos\psi-\sin b\psi-b\psi\right)\right. & \\ \left.-\left(1+\psi^2\left(\beta+\beta_1\right)\right)\sin a\psi+\psi\cos a\psi\right\} & P<0 \\ -\dfrac{WL}{\psi\Omega}\left\{\left(1-\psi^2\beta\right)\left(\left(1-\psi^2\left(\beta+b\beta_1\right)\right)\sinh\psi-a\psi\cosh\psi-\sinh b\psi-b\psi\right)\right. & \\ \left.-\left(1-\psi^2\left(\beta+\beta_1\right)\right)\sinh a\psi+\psi\cosh a\psi\right\} & P>0 \end{cases} \tag{36b}$$

Linear variation of load

In Figure 5, for example, the same uniform member is shown loaded by a total load W, which is distributed with an intensity varying linearly from w_1 at the left-hand end

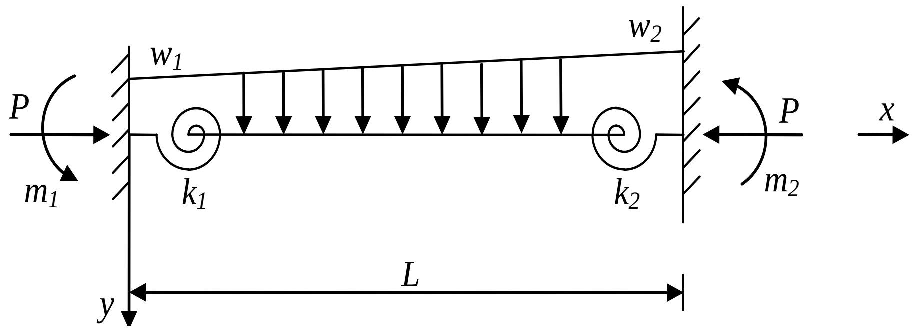

Figure 5. Linear variation of load.

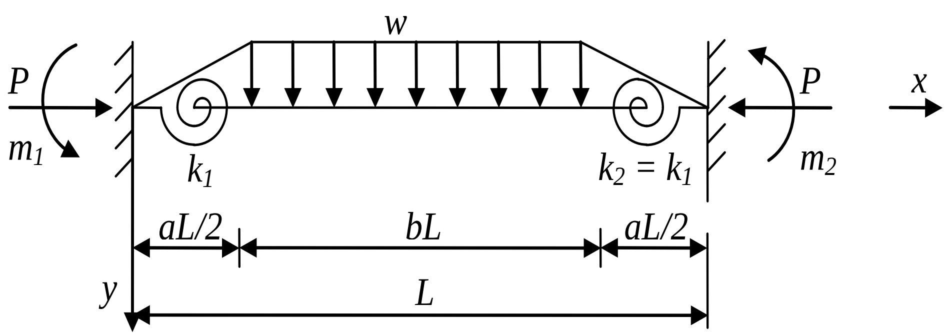

Figure 6. Symmetrical trapezoidal load.

to w_2 at the right.

$$m_1=\begin{cases}\dfrac{L^2}{60\Omega}\left\{3w_1+2w_2+30\left(w_1+w_2\right)\beta\right.\\ \left.+2\left(8w_1+7w_2\right)\beta_2\right\} & P=0\\ \dfrac{\left(w_1+w_2\right)\left(1+\psi^2\beta\right)L^2}{2\psi^2\Omega}\left\{\psi\left[4+\psi^2\left(2\beta+\beta_2\right)\right]\sin\psi\right.\\ \left.+\left[4-\psi^2\left(1-2\beta_2\right)\right]\cos\psi-\left[4+\psi^2\left(1+4\beta+2\beta_2\right)\right]\right\} & P<0\\ -\dfrac{\left(w_1+w_2\right)\left(1-\psi^2\beta\right)L^2}{2\psi^2\Omega}\left\{\psi\left[4-\psi^2\left(2\beta+\beta_2\right)\right]\sinh\psi\right.\\ \left.+\left[4-\psi^2\left(1-2\beta_2\right)\right]\cosh\psi-\left[4+\psi^2\left(1+2\beta_2\right)\right]\right\} & P>0\end{cases}\tag{37a}$$

$$m_2=-\begin{cases}\dfrac{L^2}{60\Omega}\left\{3w_2+2w_1+30\left(w_1+w_2\right)\beta\right.\\ \left.+2\left(8w_2+7w_1\right)\beta_1\right\} & P=0\\ \dfrac{\left(w_1+w_2\right)\left(1+\psi^2\beta\right)L^2}{2\psi^2\Omega}\left\{\psi\left[4+\psi^2\left(2\beta+\beta_1\right)\right]\sin\psi\right.\\ \left.+\left[4-\psi^2\left(1-2\beta_1\right)\right]\cos\psi-\left[4+\psi^2\left(1+4\beta+2\beta_1\right)\right]\right\} & P<0\\ -\dfrac{\left(w_1+w_2\right)\left(1-\psi^2\beta\right)L^2}{2\psi^2\Omega}\left\{\psi\left[4-\psi^2\left(2\beta+\beta_1\right)\right]\sinh\psi\right.\\ \left.+\left[4-\psi^2\left(1-2\beta_1\right)\right]\cosh\psi-\left[4+\psi^2\left(1+2\beta_1\right)\right]\right\} & P>0\end{cases}\tag{37b}$$

Symmetrical trapezoidal load (Figure 6)

$$m_1=\begin{cases}\dfrac{wL^2}{96}\dfrac{\left\{8+a^2\left(a-4\right)\right\}}{\left(1+2\beta_1\right)} & P=0\\ \dfrac{wL^2\left(1+\psi^2\beta\right)}{4a\psi^3}\dfrac{\left\{\left[a\psi^2\left(a-2\right)-8\right]\cos\left(\psi/2\right)+8\cos b\left(\psi/2\right)\right\}}{\sin\left(\psi/2\right)+\psi\beta_1\cos\left(\psi/2\right)} & P<0\\ -\dfrac{wL^2\left(1-\psi^2\beta\right)}{4a\psi^3}\dfrac{\left\{\left[a\psi^2\left(a-2\right)+8\right]\cosh\left(\psi/2\right)-8\cosh b\left(\psi/2\right)\right\}}{\sinh\left(\psi/2\right)+\psi\beta_1\cosh\left(\psi/2\right)} & P>0\end{cases}\tag{38a}$$

$$m_2=-\begin{cases}\dfrac{wL^2}{96}\dfrac{\left\{8+a^2\left(a-4\right)\right\}}{\left(1+2\beta_2\right)} & P=0\\ \dfrac{wL^2\left(1+\psi^2\beta\right)}{4a\psi^3}\dfrac{\left\{\left[a\psi^2\left(a-2\right)-8\right]\cos\left(\psi/2\right)+8\cos b\left(\psi/2\right)\right\}}{\sin\left(\psi/2\right)+\psi\beta_2\cos\left(\psi/2\right)} & P<0\\ -\dfrac{wL^2\left(1-\psi^2\beta\right)}{4a\psi^3}\dfrac{\left\{\left[a\psi^2\left(a-2\right)+8\right]\cosh\left(\psi/2\right)-8\cosh b\left(\psi/2\right)\right\}}{\sinh\left(\psi/2\right)+\psi\beta_2\cosh\left(\psi/2\right)} & P>0\end{cases}\tag{38b}$$

Triangular load

Determined the fixed-end moments in the uniform member shown in the Figure 7, when subjected to an unsymmetrical load, with a linear variation of intensity but of total $wL/2$.

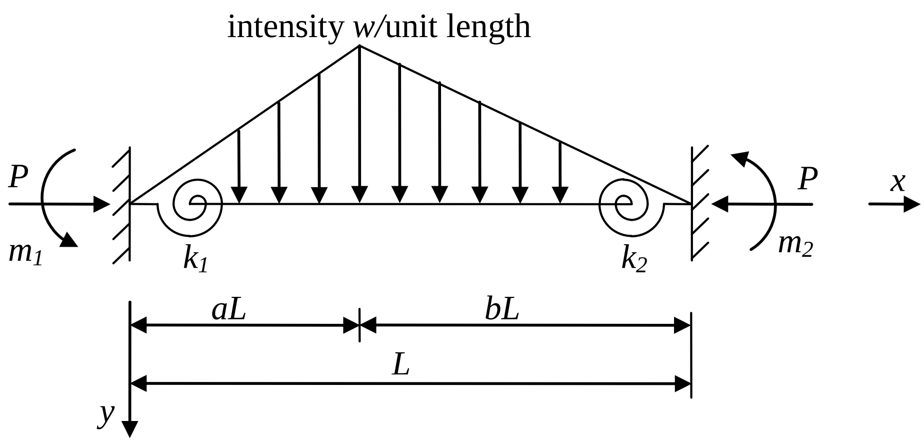

Figure 7. Triangular load.

$$m_1 = \begin{cases} \dfrac{wL^2}{60\Omega}\left\{3a^3 - 7a^2 + 3a + 3 + 30\left(ab+1\right)\beta \right. \\ \left. + \left(6a^3 - 24a^2 + 16a + 16\right)\beta_2\right\} & P = 0 \\ \dfrac{wL^2}{\psi\Omega}\left\{H1 + H2 + H3\right\} & P \neq 0 \end{cases} \quad (39a)$$

$$m_2 = -\begin{cases} \dfrac{wL^2}{60\Omega}\left\{3b^3 - 7b^2 + 3b + 3 + 30\left(ab+1\right)\beta \right. \\ \left. + \left(6b^3 - 24b^2 + 16b + 16\right)\beta_1\right\} & P = 0 \\ \dfrac{wL^2}{\psi\Omega}\left\{H1 + H2 + H3\right\} & P \neq 0 \end{cases} \quad (39b)$$

in which,

$$\left.\begin{aligned} H1 &= \left(\frac{1}{b\psi^2} + \frac{1}{3} - \frac{b}{6}\right)\left[\left(1+\psi^2\beta\right)\sin\psi - \psi\right] \\ H2 &= -\frac{1}{ab\psi^2}\left[\left(1+\psi^2\beta\right)\sin a\psi + \left(1+\psi^2\left(\beta+\beta_2\right)\right)\sin b\psi - \psi\cos b\psi\right] \\ H3 &= \left(\frac{1}{a\psi^2} + \frac{1}{3} - \frac{a}{6}\right)\left[\left(1+\psi^2\left(\beta+\beta_2\right)\right)\sin\psi - \psi\cos\psi\right] \end{aligned}\right\} P < 0 \quad (40a)$$

$$\left.\begin{aligned} H1 &= \left(\frac{1}{b\psi^2} - \frac{1}{3} + \frac{b}{6}\right)\left[\left(1-\psi^2\beta\right)\sinh\psi - \psi\right] \\ H2 &= -\frac{1}{ab\psi^2}\left[\left(1-\psi^2\beta\right)\sinh a\psi + \left(1-\psi^2\left(\beta+\beta_2\right)\right)\sinh b\psi - \psi\cosh b\psi\right] \\ H3 &= \left(\frac{1}{a\psi^2} - \frac{1}{3} + \frac{a}{6}\right)\left[\left(1-\psi^2\left(\beta+\beta_2\right)\right)\sinh\psi - \psi\cosh\psi\right] \end{aligned}\right\} P > 0 \quad (40b)$$

The remaining other two nonzero modified fixed end forces, the shear forces and the axial forces, of relevance at the ends are found using static equilibrium equations. The modified fixed end moments at the right ends for above frequently encountered loads for linear and nonlinear cases are found either from symmetry or by an interchange of a and b, β_1 and β_2 or w values at the two ends, and the sign in front of it negative.

ANALYSIS PROCEDURE

The analytical expressions having been prepared for all the quantities of relevance for the problem, it remained only to write down a computer program for numerical applications. That was done and the resulting program contains special differences compared to a linear analysis. The main difference is that there is an iteration which can be stopped when a desired accuracy is reached. The geometric stiffness matrix, as it is called, due to axial force is a relevant feature of this analysis, which actually is the cause of the necessity for the iterative procedure. The computer program analysis starts with zero axial forces in all members, giving the linear solution at the first step. It assumes the axial forces in members to be zero initially. It setups the overall stiffness matrix, analyzes the frame under the external loads, obtains joint displacements and member end forces. Then, at each new load step the axial forces and frame deflections found in the previous step are used in the computations, of both the modified stiffness matrix (calculates the corresponding stability functions) and the modified fixed end forces. The nonlinear analysis terminated when the difference between the axial forces found in two successive iterations is less than 0.1% for each member. When the predetermined precision is attained, the iteration stops and the final displacements and rotations, member end forces, and variations of bending moment along relevant members are determined. The maximum value of the bending moment in each member is given, along with the maximum value and its position on the member.

During these iterations the determinant of the overall structure stiffness matrix is calculated and loss of stability is checked. If the convergence in the axial force is obtained without loss of stability, the joint displacements and member forces obtained in this nonlinear response are used in the computation of fitness values for this individual. It should be noted that in this algorithm the design load is not applied incrementally in the nonlinear analysis. Instead it is applied immediately and iterations are carried out at this load. It should also be pointed out that during the nonlinear analysis the fixed end moments change from one iteration to another due to axial forces in the members and rotational springs attached at the ends of members. The modified fixed end moments are calculated by taking into account the effect of shear deformations and the effect of flexible end connection for a frame member which is loaded as described in Yilmaz (2008).

ANALYSIS EXAMPLE AND RESULTS

The linear and nonlinear analysis procedures are illustrated in the following example structure comprised of lintel beams having fully rigid end sections connected to wide column members (shear walls) with rigid and semi-rigid connections. The example is a shear wall with opening, a six-story single-bay building framework, the linear and nonlinear analysis of which have been extensively studied in the literature from a variety of different computational viewpoints for which analytical results found using the computer programme are compared with other analytical results (Girijavallabhan, 1969; Popov et al., 1979; Dincer, 1989).

Figure 8 shows the dimensions of the model shear wall, the connecting beams, and the assumed values of the arbitrary lateral loads. The lateral loads, assumed to be due to force of the wind acting on the side of the building, are transferred to the shear wall through cross beams placed horizontally between shear walls. The overall dimensions and loads are the same as those employed in an example problem by Girijavallabhan (1969). To simplify the analysis the modulus of elasticity of the shear walls and the connecting lintel beams are assumed to be the same, even though it was deemed feasible to assume different values of modulus of elasticity for every finite element in the assemblage (Girijavallabhan, 1969).

The bottom boundaries of the shear walls were assumed to be rigid, the bottom nodal displacements were kept equal to zero; such a boundary condition is more realistic.

The structure is a building frame that supports loads shown in Figure 8. All lintel beams and wide columns have rectangular shape sections that are oriented in the plane of the framework and are assumed to be fully restrained against out-of-plane behaviour with the following properties: lintel beams section depth h = 2ft, the thickness of the wall was assumed to be equal to 1.0 ft., section area A = 2 ft^2, moment of inertia I = 0.667 ft^4, and shape factor $f = 5/6$. Wide columns section area $A = 20\ \mathrm{ft}^2$, moment of inertia $I = 667.667\ \mathrm{ft}^4$. Poisson's ratio $\nu = 0.15$. The framework has 18 members, 14 nodes and 36 degrees-of-freedom (dof) for nodal displacement (i.e. lateral and vertical translation and rotation dof at each of the twelve free nodes 2 to 13). The members and nodes are designated by a square and a circle symbol (□, O) with a number inscribed in it that indicates the member or node number respectively, shown in Figure 9. Briefly discussed in the following are the results of the study that demonstrate analytically the influence that shear, semi-rigid connections, and the geometrically nonlinear have on the behaviour of the member end forces.

The analytical results presented in Tables 1 to 7 account for the combined influence that bending and shearing have on elastic behaviour, and were found using the computer programme to include the effect that shear deformations have on elastic behaviour. It is readily possible to conduct the same analysis using Euler-Bernoulli beam theory, which ignores the effect of shear deformation on elastic behaviour, by setting the beam-column member shear stiffness $GA_s = \infty$ in equations (2) and (4).

The analysis results found by this study are given in Tables 1 to 7 and compared with the results of other studies.

This example frame originally appeared in Girijavallabhan (1969) and, since then, its nonlinear analysis has been studied by a number of researchers from a variety of computational viewpoints; Girijavallabhan (1969) conducted finite element analysis (with 918 nodes and 1568 elements). Popov et al. (1979) also conducted finite element analysis of the frame (with 264 elements) using the program SUBWALL. Dincer (1989) analyzed the frame using a nonlinear analysis program (with 18 elements).

The linear analysis results, member end forces, found by this study are given in Table 1, and member end moments are compared with the results of other studies in Table 2 for the six lintel beams only considering the effect of shear deformation ($\nu = 0.15$). The member end forces for the beams obtained by different methods were practically the same except by Girijavallabhan (1969). The results for the method proposed herein are in exact values with Dincer (1989), in close agreement with those of Popov et al. (1979), and different from the results for the method proposed by Girijavallabhan (1969). The discrepancies between the methods are mainly due to a numerical mistake made by Girijavallabhan (1969), not due to using the simple bending theory as Popov et al. (1979) thought.

The same example were solved by increasing the Young's modulus, E, of the material with the same properties to induce the nonlinearity due to the effect of internal forces on bending.

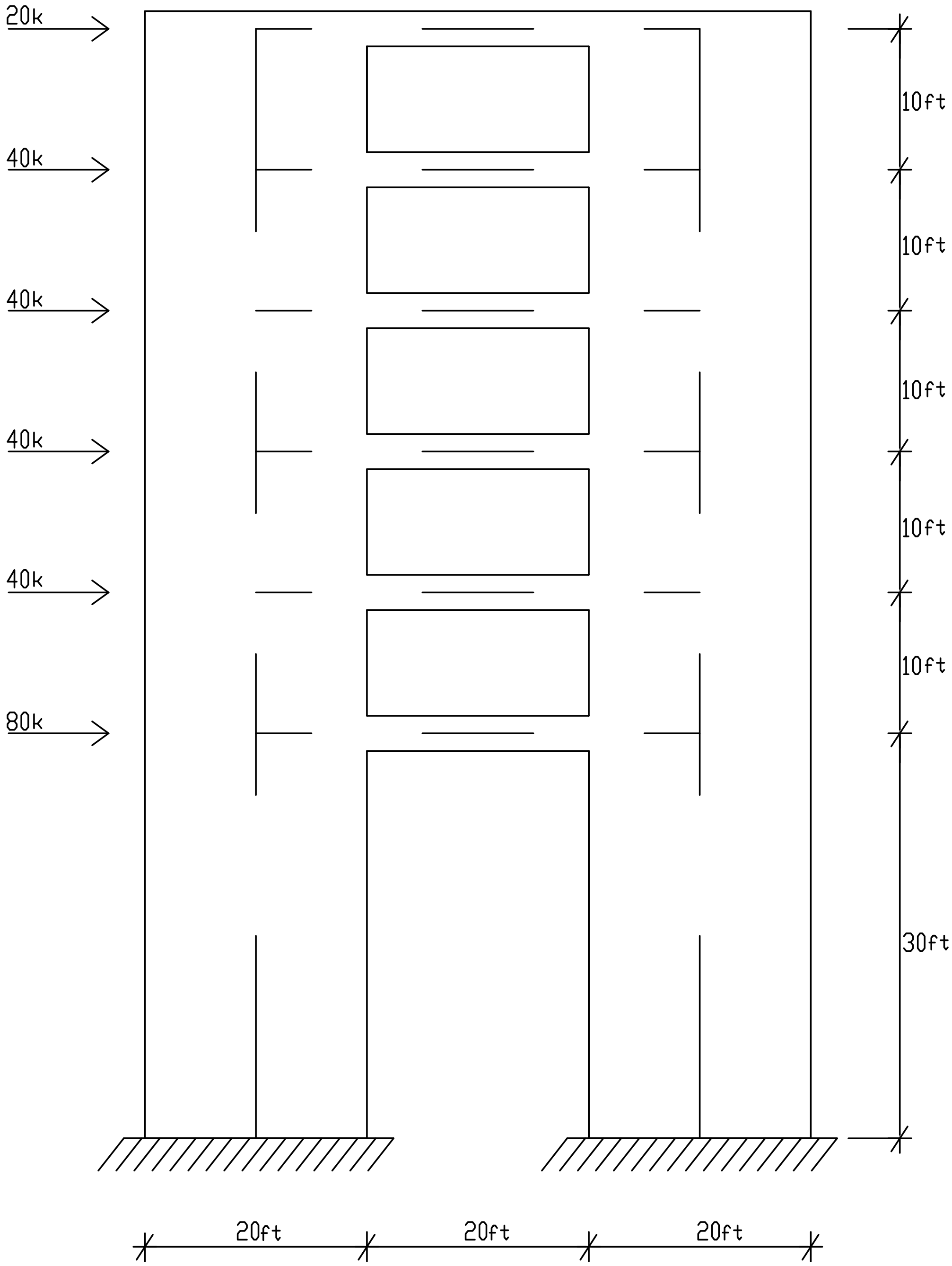

Figure 8. Model shear wall problem.

The nonlinear analysis terminated when the difference between the axial forces found in two successive iterations is less than 0.1% for each member.

The linear and nonlinear analyses results, member end forces, by increasing the Young's modulus, *E*, of the material, found by this study are given in Tables 3 and 4 neglecting the effect of shear deformation ($\nu = 0$), given in Table 5 considering the effect of shear deformation ($\nu = 0.15$), and the results of the linear and nonlinear analyses, member end moments, are compared in Table 6 for the six lintel beams of the model shear wall problem with ($\nu = 0$)/without ($\nu = 0.15$) the effect of shear deformation.

The nodal displacement vector for the given boundary forces and displacements was determined by using equation (1), developed for the complete assemblage of

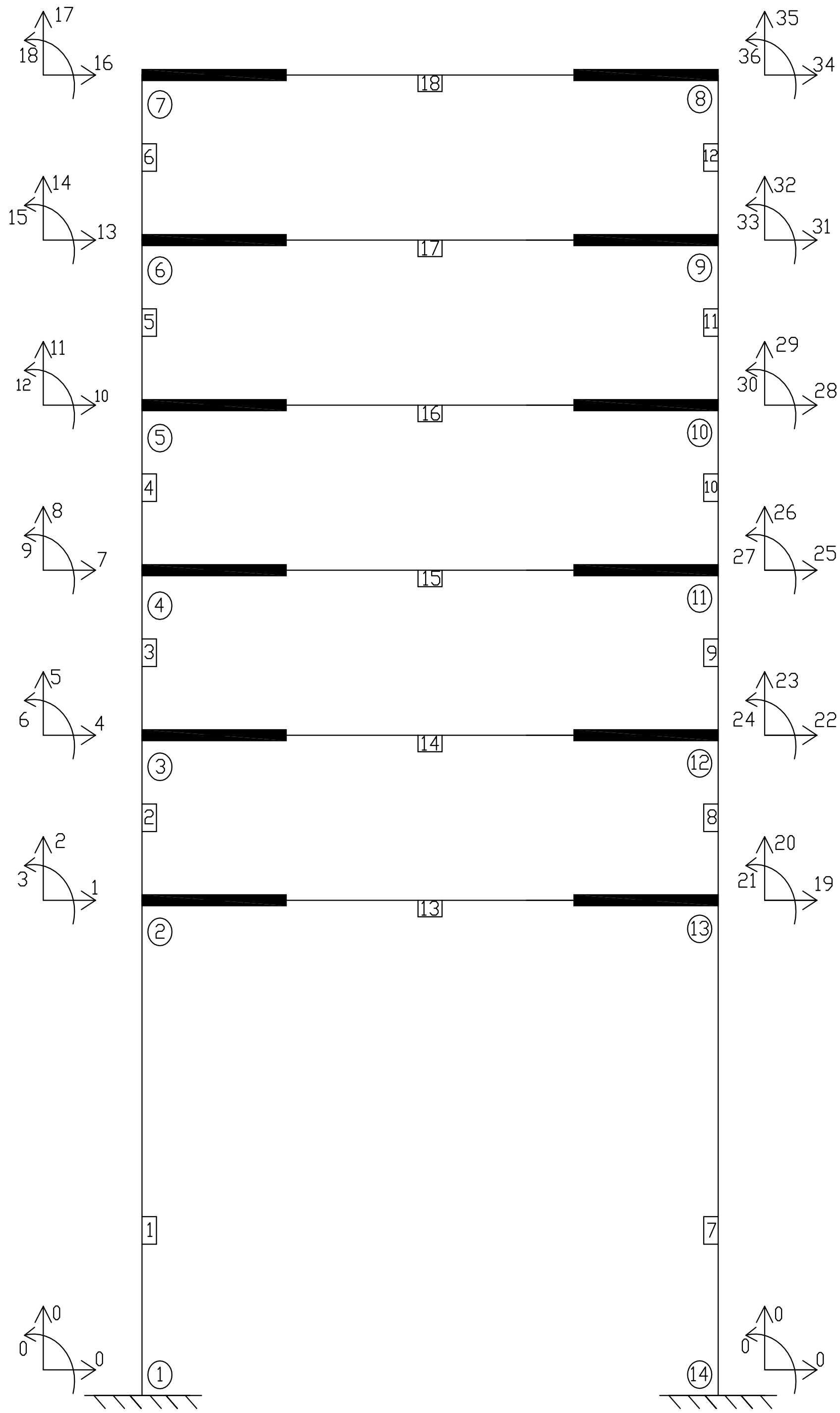

Figure 9. Coding and numbering of the example problem.

the beam-column members. The same model problem was again solved, using geometrically nonlinear analysis with and without the effect of shear deformation. The nodal displacements obtained by both analyses were compared in Table 7 for rigid joins only, and it was observed that the overall displacement pattern were different.

To give an idea about the effect of spring constants, on the displacements, the variations of the horizontal nodal displacements of left axis of the shear wall, the six nodes (joint nodes 2, 3, 4, 5, 6 and 7) of the frame are plotted in Figure 10 for the purpose of comparison. Values are

Table 1. Member end forces with rigid connections for linear frame analysis.

Member	Member end forces				
	Considering the effect of shear deformation ($\nu = 0.15$)				
	m_1 (kip-ft)	m_2 (kip-ft)	V_1 (kips)	V_2 (kips)	P (kips)
1	5763.7287	-1521.5206	141.4069	-141.4069	42.4207
2	1645.4011	-804.4833	84.0918	-84.0918	36.2329
3	943.0422	-271.1846	67.1858	-67.1858	29.3061
4	416.8724	75.7545	49.2627	-49.2627	22.0200
5	71.9143	223.1918	29.5106	-29.5106	14.6329
6	-76.3393	145.5773	6.9238	-6.9238	7.2849
7	5339.4423	-1781.6503	118.5931	-118.5931	-42.4207
8	1905.2845	-946.2023	95.9082	-95.9082	-36.2329
9	1084.7157	-356.5734	72.8142	-72.8142	-29.3061
10	502.3293	5.0438	50.7373	-50.7373	-22.0200
11	142.7712	162.1227	30.4894	-30.4894	-14.6329
12	-15.0580	145.8201	13.0762	-13.0762	-7.2849
13	-62.0018	-61.7555	-6.1879	6.1879	-22.6848
14	-69.2908	-69.2454	-6.9268	6.9268	-23.0940
15	-72.8269	-72.8950	-7.2861	7.2861	-22.0769
16	-73.7978	-73.9441	-7.3871	7.3871	-20.2479
17	-73.3732	-73.5854	-7.3479	7.3479	-17.4132
18	-72.7279	-72.9707	-7.2849	7.2849	-13.0762

Table 2. Comparison of member end moments with rigid connections for linear frame analysis

Lintel beam	Considering the effect of shear deformation ($\nu = 0.15$)					
	Girijavallabhan (1969)		Popov et al. (1979)		Dincer (1989) and present study	
	m_1 (kip-ft)	m_2 (kip-ft)	m_1 (kip-ft)	m_2 (kip-ft)	m_1(kip-ft)	m_2 (kip-ft)
13	38.78	38.48	62.70	62.50	62.00	61.76
14	41.10	40.89	69.32	69.25	69.29	69.25
15	41.33	41.06	72.26	72.35	72.83	72.90
16	40.29	39.79	72.90	73.05	73.80	73.94
17	38.75	38.27	72.17	72.37	73.37	73.59
18	31.37	31.60	61.59	62.91	72.73	72.97

given at the joints each floor level for all the nonlinear analyses with/without shear effects for $k_1 = k_2 = 0$ (pin), 0.5, 1.0 and 10^9 (rigid). The difference between the linear and nonlinear deflections for both the semi-rigid and rigid connections with and without shear effect is less than 0.096 ft over the full height of the wall. Here it is assumed that the relative rotation of the beam and the wall face at the joint would not be zero.

A drift factor of sway deflection = height/500 of the frame is defined by the continuous line in Figure 10. It can be seen that only where the semi-rigid joints are considered are the deflections less than the pin case.

Horizontal sway deflections of the six nodes (joint nodes 2, 3, 4, 5, 6 and 7) of the frame with rigid connections only are plotted in Figure 11 for all the linear and nonlinear analyses with $(\nu = 0.15)$ and without $(\nu = 0)$ shear effects. The difference between the linear and nonlinear horizontal deflections for rigid connections without shear effect is 0.0176 ft while the difference between the linear and nonlinear deflections with shear effects for rigid connections is 0.0179 over the full height of the structure. It can be seem that the effect of the shear deformations is greater than the effect of the geometric nonlinearity on the deflections for this frame example.

The member end forces were computed from nodal

Table 3. Member end forces with rigid connections for linear frame analysis.

Member	Member end forces				
	Neglecting the effect of shear deformation ($\nu = 0$)				
	***m*₁ (kip-ft)**	***m*₂ (kip-ft)**	***V*₁ (kips)**	***V*₂ (kips)**	***P* (kips)**
1	5824.0638	-1469.3156	145.1583	-145.1583	43.2861
2	1596.0024	-757.8473	83.8155	-83.8155	36.9611
3	899.3977	-240.1245	65.9273	-65.9273	29.8862
4	388.8255	94.1843	48.3010	-48.3010	22.4497
5	56.4270	233.1020	28.9529	-28.9529	14.9150
6	-83.4091	148.3445	6.4935	-6.4935	7.4242
7	5244.4935	-1799.2417	114.8417	-114.8417	-43.2861
8	1925.5538	-963.7089	96.1845	-96.1845	-36.9611
9	1105.1525	-364.4256	74.0727	-74.0727	-29.8862
10	513.1848	3.8053	51.6990	-51.6990	-22.4497
11	146.9717	163.4993	31.0471	-31.0471	-14.9150
12	-13.5606	148.6252	13.5065	-13.5065	-7.4242
13	-63.4370	-63.0624	-6.3250	6.3250	-18.6572
14	-70.8019	-70.6951	-7.0748	7.0748	-22.1118
15	-74.3359	-74.3942	-7.4365	7.4365	-22.3737
16	-75.2642	-75.4299	-7.5347	7.5347	-20.6519
17	-74.7850	-75.0308	-7.4908	7.4908	-17.5406
18	-74.1021	-74.3827	-7.4242	7.4242	-13.5065

Table 4. Member end forces with rigid connections for nonlinear frame analysis

Member	Member end forces				
	Neglecting the effect of shear deformation ($\nu = 0$)				
	***m*₁ (kip-ft)**	***m*₂ (kip-ft)**	***V*₁ (kips)**	***V*₂ (kips)**	***P* (kips)**
1	5868.3279	-1511.6259	145.6322	-145.6322	41.1532
2	1631.5414	-794.6267	84.3107	-84.3107	35.1575
3	927.1938	-268.5304	66.4068	-66.4068	28.5218
4	407.9488	75.0078	48.7157	-48.7157	21.5396
5	67.3667	222.4179	29.2600	-29.2600	14.4077
6	-79.0751	144.2800	6.6605	-6.6605	7.2268
7	5286.8834	-1844.3539	114.3678	-114.3678	-41.1532
8	1964.0363	-1001.0711	95.6893	-95.6893	-35.1575
9	1133.5805	-392.2499	73.5932	-73.5932	-28.5218
10	531.7022	-14.6209	51.2843	-51.2843	-21.5396
11	157.0943	153.1664	30.7400	-30.7400	-14.4077
12	-9.6624	144.4868	13.3395	-13.3395	-7.2268
13	-59.9585	-59.7252	-5.9957	5.9957	-18.6785
14	-66.2099	-66.1523	-6.6357	6.6357	-22.0960
15	-69.5955	-69.6294	-6.9822	6.9822	-22.3089
16	-71.0543	-71.1531	-7.1319	7.1319	-20.5443
17	-71.5329	-71.6941	-7.1809	7.1809	-17.4005
18	-72.0104	-72.2172	-7.2268	7.2268	-13.3395

displacements in all cases, and the results for the method proposed herein are in close agreement with those for all other methods except by Girijavallabhan (1969). The slight discrepancies between the methods are likely

Table 5. Member end forces with rigid connections for nonlinear frame analysis.

Member	Member end forces				
	Considering the effect of shear deformation ($\nu = 0.15$)				
	m₁ **(kip-ft)**				
1	5808.8672	-1565.6060	141.9181	-141.9181	40.2200
2	1681.0020	-841.0891	84.6388	-84.6388	34.4467
3	970.2714	-298.8287	67.7028	-67.7028	27.9792
4	435.4625	57.1800	49.6935	-49.6935	21.1364
5	82.5058	212.8324	29.8181	-29.8181	14.1397
6	-72.2553	141.7219	7.0860	-7.0860	7.0979
7	5383.6610	-1827.8358	118.0819	-118.0819	-40.2200
8	1943.0991	-983.0238	95.3612	-95.3612	-34.4467
9	1112.1834	-383.5961	72.2972	-72.2972	-27.9792
10	520.2695	-12.8725	50.3065	-50.3065	-21.1364
11	152.6467	152.0554	30.1819	-30.1819	-14.1397
12	-11.3385	141.9029	12.9140	-12.9140	-7.0979
13	-57.6627	-57.5300	-5.7733	5.7733	-22.7207
14	-64.5068	-64.4841	-6.4675	6.4675	-23.0641
15	-68.2052	-68.2448	-6.8427	6.8427	-21.9907
16	-69.7168	-69.8051	-6.9968	6.9968	-20.1246
17	-70.1582	-70.2979	-7.0418	7.0418	-17.2679
18	-70.7419	-70.9228	-7.0979	7.0979	-12.9140

Table 6. Comparison of member end moments with rigid connections for linear and nonlinear frame analyses

Lintel beam	Member end moments (kip-ft)							
	Linear $\nu = 0$		Linear $\nu = 0.15$		Nonlinear $\nu = 0$		Nonlinear $\nu = 0.15$	
	m_1	m_2	m_1	m_2	m_1	m_2	m_1	m_2
13	63.44	63.06	62.00	61.76	59.96	59.73	57.66	57.53
14	70.80	70.70	69.29	69.25	66.21	66.15	64.51	64.48
15	74.34	74.39	72.83	72.90	69.60	69.63	68.21	68.24
16	75.26	75.43	73.80	73.94	71.05	71.15	69.72	69.81
17	74.79	75.03	73.37	73.59	71.53	71.69	70.16	70.30
18	74.10	74.38	72.73	72.97	72.01	72.22	70.74	70.92

mainly due to different ways in which the member fixed end forces are considered. It is worth noting that the structural model for the proposed method involved significantly fewer beam and column elements (only 18 elements) than the other methods.

Conclusion

Analysis by conventional simple bending theories might lead to an overestimation or underestimation of the end forces in shear walls and lintel beams. In this study the second order analysis of planar frames made up of flexibly connected prismatic members having rigid end sections taking into consideration the effect of shear deformations is considered and a computer program is prepared for numerical computations. Different types of span loadings are considered and most of the span loadings not being found in the literature, the results are checked among themselves as special cases of others. Moreover, special problems being mirror images of others are used for checking purposes, as well. A design example is included to demonstrate effect of connection flexibility, rigid end sections, shear deformations and the geometrical nonlinearity in the design of general frames.

It is noticed from the design example that semi-rigid connection flexibility affects the distribution of forces in the frame and causes increase in the drift of the frame.

Table 7. Comparison of joint displacements with rigid connections for nonlinear frame analysis

Displacement no.	Joint displacements lateral and vertical translations (ft), rotations (radians)	
	Neglecting the effect of shear deformation ($\nu = 0$)	Considering the effect of shear deformation ($\nu = 0.15$)
	Nonlinear analysis Nonlinear Linear Nonlinear	
1	0.2980848455972192	0.3551806822627144
2	6.172982981319033D-03	6.033000919717811D-03
3	-1.660481286579463D-02	-1.659248179035046D-02
4	0.4742771973768766	0.5432039793290816
5	7.930858378012861D-03	7.755334416486581D-03
6	-1.842442986664716D-02	-1.848404070014761D-02
7	0.6638287644835048	0.7429086977084692
8	9.356950110235815D-03	9.154293412705168D-03
9	-1.932121854344592D-02	-0.0194358610389928
10	0.8588931652910163	0.9461001264057282
11	1.043393167278179D-02	1.021111535164722D-02
12	-1.957092304760685D-02	-1.971957148346693D-02
13	1.054383185616977	1.147251957969186
14	1.115431766190441D-02	1.091809875859807D-02
15	-1.945463523729933D-02	-1.962182699973432D-02
16	1.248173466413118	1.343713289352048
17	1.151566006402824D-02	1.127299343405697D-02
18	-0.019287119775222	-1.946134495756661D-02
19	0.2794063214754065	0.3324600230060343
20	-6.172982981319009D-03	-6.033000919717824D-03
21	-1.604520388960615D-02	-1.622578665999867D-02
22	0.4521811577959595	0.520139922248268
23	-7.930858378012828D-03	-0.0077553344164866
24	-1.826902327624582D-02	-1.842036783532534D-02
25	0.641519884590283	0.7209179795774135
26	-9.356950110235776D-03	-9.154293412705192D-03
27	-0.019413390360414	-1.954219686659011D-02
28	0.8383488381865102	0.9259755420668144
29	-1.043393167278175D-02	-1.021111535164725D-02
30	-0.0198231306809694	-1.994205135957471D-02
31	1.036982698164563	1.129984037771627
32	-1.115431766190437D-02	-1.091809875859811D-02
33	-1.982607652613628D-02	-1.994249479714114D-02
34	1.234833936257369	1.330799325476182
35	-1.151566006402821D-02	-1.127299343405701D-02
36	-1.971046515581687D-02	-0.0198275643243373

This in turn necessitates the consideration of $P-\Delta$ effect in the frame analysis. It required three to five iterations in the design examples considered to obtain the nonlinear response of frame which clearly indicates the significance of geometric nonlinearity in the analysis and design of semi-rigid frames. It is also noticed that consideration of $P-\Delta$ effect and shear deformation yields a heavier frame in the case of semi-rigid as well as rigid frame. The analysis example demonstrate that the proposed nonlinear analysis method based on bending, shearing and axial stiffness approximately simulates the elastic behaviour of structures. Comparisons with results found by other methods for the frame example determined that the proposed method can effectively predict the member end forces of general frameworks, achieve more accurate results than the conventional

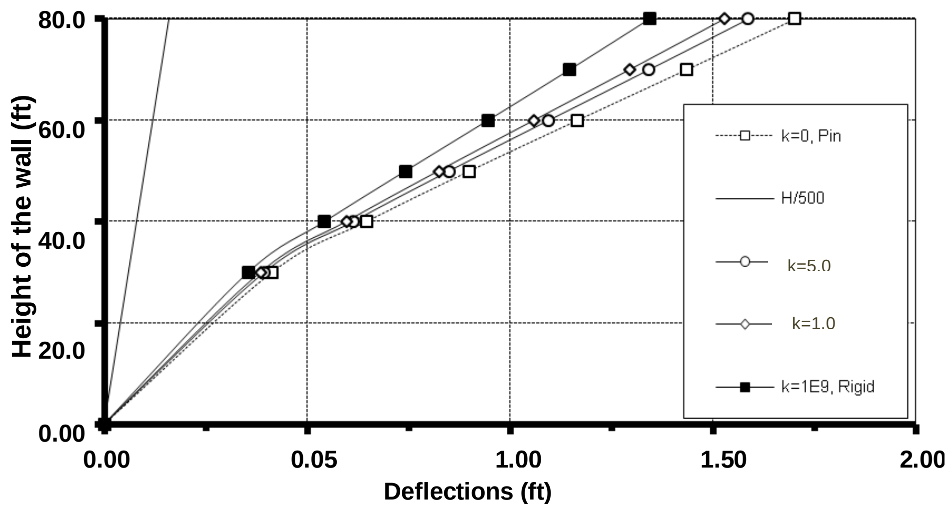

Figure 10. Lateral deflections at each floor level in the example problem with varying spring constants k.

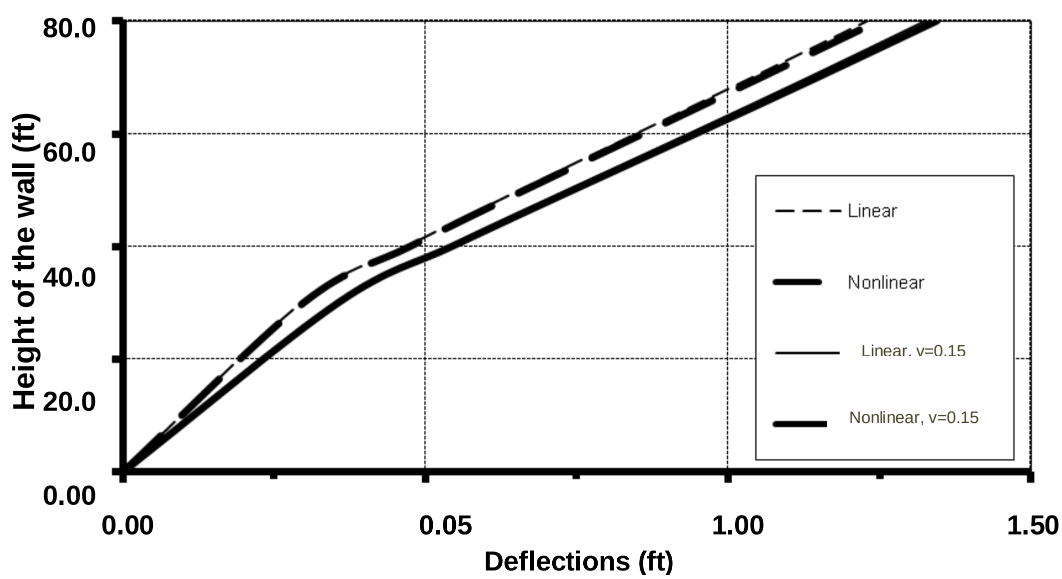

Figure 11. Lateral deflections at each floor level in the example problem with rigid connections.

method.

It has also been observed that displacements and critical extreme values of bending moment for the same structure become larger when the spring constants of flexible connections become less. The variation is between the values pertaining to simple, $k_1 = k_2 = 0$ (pin), and rigid, $k_1 = k_2 = \infty$ (rigid), end connections.

Compared to other approaches, the primary advantages of the proposed method are its simplicity, practicality and efficiency. The proposed stiffness coefficients simplify the means to account for geometric nonlinearity, effect of shear deformation, rigid end sections, and semi-rigid connections. Finally, studies have shown that the proposed method can be readily and effectively implemented for the advanced analysis and design of steel frames, especially, nowadays, widely used precast reinforced concrete structures, and structure comprised of lintel beams having fully rigid end sections connected to wide column members (shear walls) with rigid and semi-rigid connections.

ACKNOWLEDGEMENT

This work forms part of the M.Sc research studies conducted by the second and third authors under the supervision of the first author. The authors wish to express their appreciation to the Department of Civil Engineering of Dicle University for providing computer facilities during the investigation.

REFERENCES

Al-Sarraf SZ (1986). Shear effect on the elastic stability of frames. Struct. Eng. 64B(2):43-47.

Aristizabal-Ochoa D (2012). Matrix method for stability and second-order analysis of Timoshenko beam-column structures with semi-rigid connections. J. Eng. Struct. 34:289-302.

Chan SL, Zhau ZH (1994). A pointwise equilibrating polynomial (PEP) element for nonlinear analysis frames. J. Struct. Eng. ASCE. 120(6):1703-17.

Chen WF, Lui EM (1991). Stability design of steel frames. Florida: Boca Raton:CRC Press.

Dincer R (1989). Nonlinear analysis of planar frames with linear prismatic members having rigid end sections taking shear deformation into consideration. M.Sc Thesis, University of Cukurova, Adana, Turkey.

Frye MJ, Morris GA (1975). Analysis of flexibly connected steel frames. Can. J. Civil Eng. 2(3):280-91.

Girijavallabhan CV (1969). Analysis of shear wall with openings. J. Struct. Div. ASCE 95(10):2093-2103.

Gorgun H (1992). The nonlinear analysis of planar frames composed of flexibly connected members. M.Sc Thesis, University of Cukurova, Adana, Turkey.

Hall WJ, Newmark NM (1957). Shear deflection of wide-flange steel beams in the plastic range. ASCE Trans. 122: 666-87.

Jones SW, Kirby PA, Nethercot DA (1983). The analysis of frames with semi-rigid connections-a state of the art report. J. Constr. Steel Res. 3(2):2-13.

Kameshki ES, Saka MP (2003). Genetic algorithm based optimum design of nonlinear planar steel frames with various semi-rigid connections. J. Constr. Steel Res. 59:109-134.

Livesley RK, Chandler DB (1956). Stability functions for structural frameworks. Manchester: Manchester University Press.

Monforton GR, Wu TS (1963). Matrix analysis of semi-rigidly connected frames. J. Struct. Div. ASCE 89(ST6):13-42.

Moree DB, Nethercot DA, Kirby PA (1993). Testing steel frames at full scale: appraisal of results and implications for design. Struct. Eng. 71:428-435.

Mottram JT (2008). Stability analysis for pitched portal frames of fibre reinforced polymer. Proceedings of the 4th International Conference on FRP Composites in Civil Engineering (CICE 2008), Empa, Dübendorf p. 6.

Popov EP, Petersson H, Le DQ (1979). Program Subwall, Finite element analysis of structural walls. ACI J. 76(30):679-696.

Romstad KM, Subramanian CV (1970). Analysis of frames with partial connection rigidity. J. Struct. Eng. ASCE 96(ST11):2283-2300.

Sekulovic M, Salatic R, Nefovska M (2002). Dynamic analysis of steel frames with flexible connections. J. Comput. Struct. 80:935-955.

Simoes LMC (1996). Optimization of frames with semi-rigid connections. Comput. Struct. 60(4):531-9.

Timoshenko SP, Gere JM (1961). Theory of elastic stability. 2nd ed. New York:McGraw-Hill.

Wu FS, Chen WF (1990). A design model for semi-rigid connections. Eng. Struct. 12(2):88-97.

Yilmaz S (2008). The nonlinear analysis of frames with semi-rigid connections and shear deformations, MSc thesis, University of Dicle, Diyarbakir, Turkey.

Yu CH, Shanmugam NE (1986). Stability of frames with semi-rigid joints. J. Comput. Struct. 23(5):639-648.